Inorg. Chem. **2005**, *44*, 3960–3971

Synthesis and Crystallographic Characterization of Low-Dimensional and Porous Coordination Compounds Capable of Supramolecular Aromatic Interaction Using the 4,4′-Azobis(pyridine) Ligand

Shin-ichiro Noro,*[,†,‡] Susumu Kitagawa,[§] Takayoshi Nakamura,[†,‡] and Tatsuo Wada[||]

Research Institute for Electronic Science, Hokkaido University, Sapporo 060-0812, Japan, Graduate School of Environmental Earth Science, Hokkaido University, Sapporo 060-0812, Japan, Department of Synthetic Chemistry and Biological Chemistry, Graduate School of Engineering, Kyoto University, Katsura, Nishikyo-ku, Kyoto 615-8510, Japan, and Supramolecular Science Laboratory, RIKEN (The Institute of Physical and Chemical Research), 2-1 Hirosawa, Wako-shi, Saitama 351-0198, Japan

Received November 18, 2004

Coordination compounds with a 4,4′-azobis(pyridine) (azpy) ligand, $\{[M_2(azpy)_6(H_2O)_5]\cdot 4PF_6\cdot azpy\cdot H_2O\}_n$ (M = Ni^{II} (**1**) or Co^{II} (**2**)) (0-dimensional (0-D) dimer), $\{[Zn(azpy)_3(H_2O)_2]\cdot 2PF_6\cdot 2azpy\cdot 4H_2O\}_n$ (**3**) (1-dimensional (1-D) fishbone-type chain), $\{[Ag(azpy)]\cdot PF_6\}_n$ (**4**) (1-D linear chain), $\{[Mn(NCS)_2(azpy)_2]\cdot azpy\}_n$ (**5**) (2-dimensional (2-D) grid sheet), and $\{[Ni(NCS)_2(azpy)_2]\cdot 3toluene\}_n$ (**6**) (2-D grid sheet), were synthesized and structurally characterized. Compounds **1** and **2** have a 0-D dimer motif, in which one M^{II} (M^{II} = Ni^{II} or Co^{II}) coordination site is shared by unidentate azpy and H_2O ligands, each with half-occupancy, i.e., exhibiting static disorder. Compounds **3** and **4** afford 1-D fishbone-type and 1-D linear chain motifs, respectively. Azpy mediates π–π and π–p interactions between these low-dimensional structures. Compounds **5** and **6** possess a 2-D grid sheet motif. These sheets assemble to form microporous frameworks that incorporate aromatic guests, such as coordination-free azpy (**5**) and toluene (**6**). There exist not only π–π and π–p interactions but also CH–π interactions between the framework azpy ligands and guests. It should be noted that the azpy ligand is a good candidate for the construction of new assembling systems of coordination compounds through its aromatic interactions.

Introduction

A new class of porous materials, known as coordination polymers, which are constructed from transition metal ions and organic bridging ligands, have attracted a great deal of attention recently. Considerable research effort has been devoted to the development, design, and synthesis of novel porous metal−organic frameworks.[1] In coordination polymers, supramolecular contacts such as hydrogen bonds and aromatic interactions contribute strongly to the formation of not only host−guest assemblies but also dynamic frameworks.

There are almost always guest molecules present within the channels or cavities of porous compounds. It is well-known that guest molecules act as template units for the construction of porous materials. Also, guest molecules incorporated into the pores must be readily removable for the resulting vacant pores to be useful in applications. Therefore, one of the rational methods to create a porous material is to introduce weak host−guest forces, that is, supramolecular interactions. In a different approach, one attempts to construct porous coordination compounds from low-dimensional (0-D, 1-D, and 2-D) motifs through weak

* Author to whom correspondence should be addressed. E-mail: noro@es.hokudai.ac.jp.
† Research Institute for Electronic Science, Hokkaido University.
‡ Graduate School of Environmental Earth Science, Hokkaido University.
§ Kyoto University.
|| RIKEN.

(1) (a) Kitagawa, S.; Noro, S. In *Comprehensive Coordination Chemistry II: From Biology to Nanotechnology*; McCleverty, J. A., Meyer, T. J., Eds.; Pergamon Press: Oxford, U.K., 2003; Vol. 7, pp 231−261. (b) Kitagawa, S.; Kitaura, R.; Noro, S. *Angew. Chem., Int. Ed.* **2004**, *43*, 2334. (c) Oh, M.; Carpenter, G. B.; Sweigart, D. A. *Acc. Chem. Res.* **2004**, *37*, 1. (d) Yaghi, O. M.; O'Keeffe, M.; Ockwig, N. W.; Chae, H. K.; Eddaoudi, M.; Kim, J. *Nature* **2003**, *423*, 705. (e) Janiak, C. *J. Chem. Soc., Dalton Trans.* **2003**, 2781. (f) James, S. L. *Chem. Soc. Rev.* **2003**, *32*, 276. (g) Moulton, B.; Zaworotko, M. J. *Curr. Opin. Solid State Mater. Sci.* **2002**, *6*, 117. (h) Kim, K. *Chem. Soc. Rev.* **2002**, *31*, 96. (i) Evans, O. R.; Lin, W. *Acc. Chem. Res.* **2002**, *35*, 511. (j) Moulton, B.; Zaworotko, M. J. *Chem. Rev.* **2001**, *101*, 1629. (k) Kesanli, B.; Lin, W. *Coord. Chem. Rev.* **2003**, *246*, 305.

10.1021/ic048371u CCC: $30.25
Published on Web 04/28/2005

Chart 1

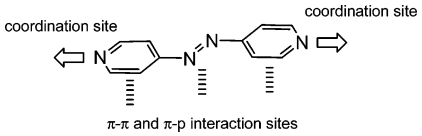

supramolecular contacts, creating a dynamic framework which could respond to external stimuli.[1b,2] While hydrogen bonds are a frequently encountered supramolecular interaction used in the construction of frameworks and host−guest assemblies, examples of such systems exploiting aromatic interactions (e.g., $\pi-\pi$, CH$-\pi$) are extremely limited. The understanding and application of aromatic interactions between host frameworks, and between host framework and aromatic guest, are of fundamental importance for the further development of porous coordination compounds. For instance, some microporous coordination polymers are able to store hydrogen at a capacity unmatched by other materials.[3] It is believed that favorable interactions exist between aromatic rings of porous frameworks and hydrogen molecules.[4] A microporous coordination polymer, $[Cu(dhbc)_2(4,4'\text{-bpy})]\cdot H_2O\}_n$ (dhbc = 2,5-dihydroxybenzoate, 4,4′-bpy = 4,4′-bipyridine), is one recent successful example in which dynamic behavior was regulated by supramolecular $\pi-\pi$ interactions.[2a] Each 2-D motif constructed from Cu^{II} connectors and dhbc and 4,4′-bpy linkers had interlocking ridges and hollows supported by the dhbc benzene rings, which undergo $\pi-\pi$ interactions. Structural transformation triggered not only by the original H_2O guest but also by a supercritical gas (which only exhibited weak dispersive interactions in this system) was facilitated by the unusual flexibility of the framework resulting from the displacement of $\pi-\pi$ interactions.

One useful strategy to create assemblies of coordination compounds supported by aromatic interactions is to employ a ligand capable of coordinating to a metal ion and participating in supramolecular aromatic interactions. Multidentate ligands with pyridine groups or nitrogen heterocycles, which generally feature as building blocks in the design of coordination frameworks and as electron-poor ring systems, tend to form stronger $\pi-\pi$ interactions than benzene and arenes.[5] A metal coordinated to a nitrogen atom will further enhance the electron-withdrawing effect through its positive charge. Hence, aromatic nitrogen heterocycles should in principle be well suited for $\pi-\pi$ interactions because of their low π-electron density.

We therefore focused on the 4,4′-azobis(pyridine) (azpy) ligand (Chart 1), which has not only metal-bridging sites but also redox and optical properties introduced by the azo (−N=N−) group.[6] Furthermore, this group provides molecular planarity by extending the π-conjugated system and p-orbitals, which facilitate formation of $\pi-\pi$ interactions with other coordinated azpy ligands or aromatic guests and concomitant $\pi-$p overlap between aromatic rings and azo moieties.[5] Thus, the azpy ligand is a good candidate for the construction of supramolecular assemblies based on aromatic interactions. We and other groups have previously reported the structures of coordination polymers with azpy ligands,[6a,7,8] and many exhibited $\pi-\pi$ and $\pi-$p interactions between these ligands. For example, the 1-D coordination polymer $\{[Fe(NCS)_2(azpy)(MeOH)_2]\cdot azpy\}_n$, with a 2-D undulated layer structure, formed infinite $\pi-\pi$ and $\pi-$p interactions between coordinated and hydrogen-bonding azpy molecules.[6a] However, detailed discussions of aromatic interactions have not been presented for the azpy system. Here we report the synthesis, crystal structures, and details regarding aromatic interactions of coordination compounds containing the azpy ligand, 0-D dimer $\{[M_2(azpy)_6(H_2O)_5]\cdot 4PF_6\cdot azpy\cdot H_2O\}_n$ (M = Ni^{II} (**1**) and Co^{II} (**2**)), 1-D fishbone-type chain $\{[Zn(azpy)_3(H_2O)_2]\cdot 2PF_6\cdot 2azpy\cdot 4H_2O\}_n$ (**3**), 1-D linear chain $\{[Ag(azpy)]\cdot PF_6\}_n$ (**4**), and 2-D grid sheet structures $\{[Mn(NCS)_2(azpy)_2]\cdot azpy\}_n$ (**5**) and $\{[Ni(NCS)_2(azpy)_2]\cdot 3toluene\}_n$ (**6**) (Scheme 1), all of which showed a rich variety of azpy-mediated $\pi-\pi$ and $\pi-$p interactions, as expected.

Experimental Section

Materials. All chemicals and solvents used during synthesis were reagent grade. 4,4′-Azobis(pyridine) ligand was prepared according to a literature method.[9]

Caution! *Perchlorate salts are explosive (especially if they are dry) and should be handled with care.*

Syntheses of $\{[M_2(azpy)_6(H_2O)_5]\cdot 4PF_6\cdot azpy\cdot H_2O\}_n$ (M = Ni^{II} (1) and Co^{II} (2)). The Ni^{II} compound was synthesized as follows: An ethanol solution (10 mL) of azpy (0.100 mg, 0.543 mmol) was added to an aqueous solution (10 mL) containing a mixture of $Ni(ClO_4)_2\cdot 6H_2O$ (0.100 g, 0.272 mmol) and NH_4PF_6 (0.089 g, 0.543 mmol) at room temperature. The resulting red solution was allowed to stand for a few days, and the red crystals obtained were collected by filtration, washed with ethanol, and dried under reduced pressure.

(2) (a) Kitaura, R.; Seki, K.; Akiyama, G.; Kitagawa, S. *Angew. Chem., Int. Ed.* **2003**, *42*, 428. (b) Takamizawa, S.; Nakata, E.; Saito, T. *Angew. Chem., Int. Ed.* **2004**, *43*, 1368. (c) Uemura, K.; Kitagawa, S.; Kondo, M.; Fukui, K.; Kitaura, R.; Chang, H.-C.; Mizutani, T. *Chem.—Eur. J.* **2002**, *8*, 3587.
(3) (a) Rosi, N. L.; Eckert, J.; Eddaoudi, M.; Vodak, D. T.; Kim, J.; O'Keeffe, M.; Yaghi, O. M. *Science* **2003**, *300*, 1127. (b) Kesanli, B.; Cui, Y.; Smith, M. R.; Bittner, E. W.; Bockrath, B. C.; Lin, W. *Angew. Chem., Int. Ed.* **2005**, *44*, 72.
(4) Nechaev, Y. S.; Alexeeva, O. K. *Int. J. Hydrogen Energy* **2003**, *28*, 1433.
(5) Janiak, C. *J. Chem. Soc., Dalton Trans.* **2000**, 3885.
(6) (a) Noro, S.; Kondo, M.; Ishii, T.; Kitagawa, S.; Matsuzaka, H. *J. Chem. Soc., Dalton Trans.* **1999**, 1569. (b) Sun, S.-S.; Lees, A. J. *J. Am. Chem. Soc.* **2000**, *122*, 8956. (c) Haladjian, J.; Pilard, R.; Bianco, P.; Asso, L. *Electrochim. Acta* **1985**, *30*, 695.
(7) (a) Kondo, M.; Shimamura, M.; Noro, S.; Yoshitomi, T.; Minakoshi, S.; Kitagawa, S. *Chem. Lett.* **1999**, 285. (b) Kondo, M.; Shimamura, M.; Noro, S.; Minakoshi, S.; Asami, A.; Seki, K.; Kitagawa, S. *Chem. Mater.* **2000**, *12*, 1288. (c) Maji, T. K.; Uemura, K.; Chang, H.-C.; Matsuda, R.; Kitagawa, S. *Angew. Chem., Int. Ed.* **2004**, *43*, 3269.
(8) (a) Withersby, M. A.; Blake, A. J.; Champness, N. R.; Cooke, P. A.; Hubberstey, P.; Schröder, M. *New J. Chem.* **1999**, *23*, 573. (b) He, C.; Zhang, B.-G.; Duan, C.-Y.; Li, J.-H.; Meng, Q.-J. *Eur. J. Inorg. Chem.* **2000**, 2549. (c) Li, B.; Lang, J.; Ding, J.; Zhang, Y. *Inorg. Chem. Commun.* **2003**, *6*, 141. (d) Halder, G. J.; Kepert, C. J.; Moubaraki, B.; Murray, K. S.; Cashion, J. D. *Science* **2002**, *298*, 1762. (e) Li, B.; Yin, G.; Cao, H.; Liu, Y.; Xu, Z. *Inorg. Chem. Commun.* **2001**, *4*, 451. (f) Tang, J.-K.; Zhu, L.-N.; Li, X.-Z.; Dong, W.; Liao, D.-Z.; Jiang, Z.-H.; Yan, S.-P.; Cheng, P. Z. *Anorg. Allg. Chem.* **2003**, *629*, 2000. (g) Moliner, N.; Muñoz, M. C.; Real, J. A. *Inorg. Chem. Commun.* **1999**, *2*, 25. (h) Li, B.; Liu, H.; Xu, Y.; Chen, J.; Xu, Z. *Chem. Lett.* **2001**, 902. (i) Li, B.; Lang, J.; Ding, J.; Zhang, Y. *Inorg. Chem. Commun.* **2003**, *6*, 141.
(9) Brown, E. V.; Granneman, G. R. *J. Am. Chem. Soc.* **1975**, *97*, 621.

Scheme 1

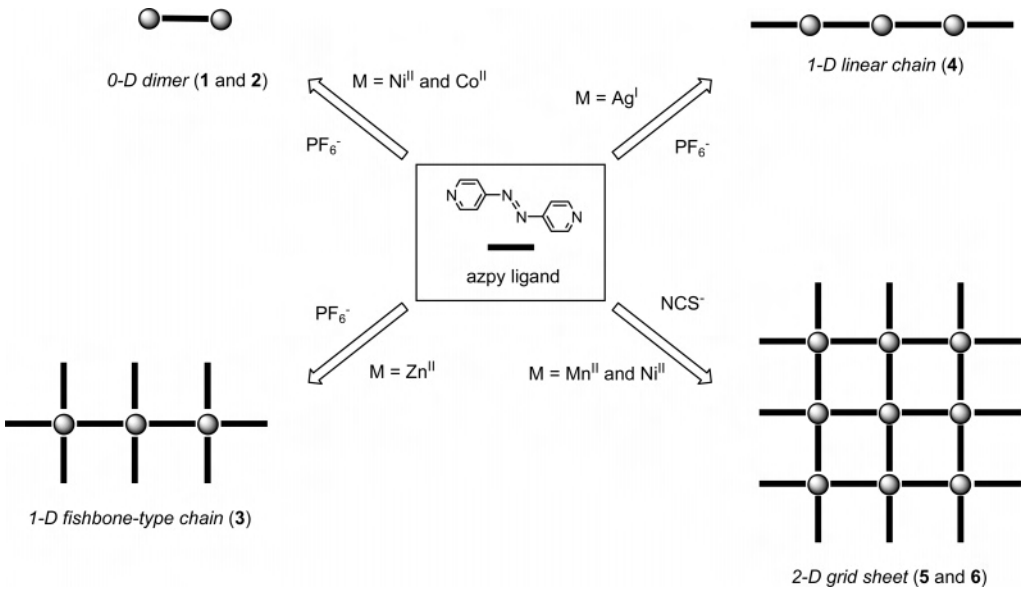

Yield: 0.119 g (0.057 mmol, 72%). Anal. Calcd for $C_{70}H_{68}F_{24}N_{28}Ni_2O_6P_4$: C, 40.14; H, 3.27; N, 18.72. Found: C, 40.31; H, 3.24; N, 18.92. IR (KBr pellet) (cm^{-1}): 3079 bm, 1598 m, 1571 m, 1492 w, 1417 m, 1324 w, 1226 m, 1191 w, 1106 w, 1049 m, 1014 m, 842 s, 738 m, 573 m, 557 m, 545 m, 527 m. The Co^{II} compound **2** was synthesized by a procedure similar to that employed for **1**; $Co(ClO_4)_2 \cdot 6H_2O$ was used instead of $Ni(ClO_4)_2 \cdot 6H_2O$. Yield: 52%. Anal. Calcd for $C_{70}H_{68}Co_2F_{24}N_{28}O_6P_4$: C, 40.13; H, 3.27; N, 18.72. Found: C, 40.31; H, 3.20; N, 18.91. IR (KBr pellet) (cm^{-1}): 3081 bm, 1597 s, 1569 m, 1491 w, 1416 s, 1324 w, 1225 m, 1190 w, 1108 w, 1050 m, 1011 m, 839 s, 739 m, 572 m, 557 s, 544 m, 528 m.

Synthesis of $\{[Zn(azpy)_3(H_2O)_2]\cdot 2PF_6\cdot 2azpy\cdot 4H_2O\}_n$ (3). An ethanol solution (5 mL) of azpy (0.046 mg, 0.250 mmol) was added to an aqueous solution (5 mL) containing a mixture of $Zn(ClO_4)_2 \cdot 6H_2O$ (0.047 g, 0.125 mmol) and NH_4PF_6 (0.163 g, 0.500 mmol) at room temperature. The resulting mixture was heated for 0.5 h, filtered, and allowed to stand for a few days. Red crystals containing **3** and another crystalline compound were collected by filtration, washed with ethanol, and dried under reduced pressure. **3** was partially separated from this mixture by hand.[10] Anal. Calcd for $C_{50}H_{52}F_{12}N_{20}O_6P_2Zn$: C, 43.38; H, 3.79; N, 20.23. Found: C, 43.22; H, 3.61; N, 20.32. IR (KBr pellet) (cm^{-1}): 3611 m, 3096 bm, 1606 s, 1589 s, 1567 m, 1490 w, 1415 s, 1323 w, 1239 w, 1225 m, 1193 w, 1095 w, 1083 w, 1053 m, 1027 m, 1017 m, 991 m, 964 w, 834 s, 739 m, 568 s, 559 s, 524 m.

Synthesis of $\{[Ag(azpy)]\cdot PF_6\}_n$ (4). An ethanol solution (10 mL) of azpy (50 mg, 0.272 mmol) was added to an aqueous solution (10 mL) of $AgPF_6$ (69 mg, 0.272 mmol) at room temperature. The pale orange powder obtained was filtered off, washed with ethanol, and dried under reduced pressure. Yield: 0.114 g (0.261 mmol, 96%). Anal. Calcd for $C_{10}H_8AgF_6N_4P$: C, 27.48; H, 1.85; N, 12.82. Found: C, 27.76; H, 2.14; N, 13.51. IR (KBr pellet) (cm^{-1}): 3117 w, 3057 w, 1604 m, 1568 w, 1496 w, 1427 m, 1232 w, 1062 w, 1030 w, 889 m, 831 s, 738 w, 669 w, 576 w, 555 m, 526 w.

Single crystals suitable for X-ray analysis were prepared by a slow diffusion of an ethanol solution of azpy into an aqueous solution of $AgPF_6$.

(10) We could not completely separate two kinds of crystalline materials. Therefore, the yield was not shown.

Synthesis of $\{[Mn(NCS)_2(azpy)_2]\cdot azpy\}_n$ (5). An ethanol solution (100 mL) of azpy (0.184 g, 1.00 mmol) was added to an aqueous solution (100 mL) containing a mixture of $Mn(ClO_4)_2 \cdot 6H_2O$ (0.120 g, 0.33 mmol) and NH_4SCN (0.051 g, 0.67 mmol) at room temperature. After the resulting red solution was allowed to stand for a few weeks, the red crystals obtained were collected by filtration, washed with ethanol, and dried under reduced pressure. Yield: 0.035 g (0.048 mmol, 15%). Anal. Calcd for $C_{32}H_{24}MnN_{14}S_2$: C, 53.11; H, 3.34; N, 27.10. Found: C, 53.00; H, 3.41; N, 27.00. IR (KBr pellet) (cm^{-1}): 3040 w, 2042 s, 1599 s, 1566 m, 1489 w, 1414 m, 1323 w, 1248 w, 1221 m, 1051 w, 1008 m, 989 w, 976 w, 854 m, 844 m, 569 m, 544 w, 526 w, 486 w.

Synthesis of $\{[Ni(NCS)_2(azpy)_2]\cdot 3toluene\}_n$ (6). Single crystals suitable for X-ray analysis were prepared by a careful diffusion of a methanol solution containing a mixture of $Ni(ClO_4)_2 \cdot 6H_2O$ and NH_4SCN into a toluene solution of azpy at room temperature. Red crystals were obtained after a few weeks. Unfortunately, a pure sample of **6** was not isolated due to contamination by another low-crystalline product.

X-ray Diffraction (XRD) Measurement. The XRD pattern of a powder sample of **4** was in good agreement with the simulated pattern reproduced from the F_c values of the calculated structure, indicative of identity of powder and crystalline samples.

Physical Techniques. Elemental analyses (C, H, N) were performed on a Yanaco C,H,N Corder MT-5. IR spectra (400−4000 cm^{-1}) were recorded on a Hitachi I-5040 FT-IR spectrometer with samples prepared as KBr pellets. XRD data were collected on a MAC Science MXP18 automated diffractometer using Cu Kα radiation.

Crystal Structure Determination. The X-ray diffraction measurements of single crystals of **1** and **2** were carried out at both room temperature (RT) and low temperature (LT). Suitable crystals were mounted on a glass fiber and coated with epoxy resin. Data were collected on a Rigaku AFC7R diffractometer (**1**(RT) and **5**), a Rigaku RAXIS-RAPID imaging plate diffractometer (**1**(LT), **2**(RT), **2**(LT), and **3**), a Rigaku RAXIS-IV imaging plate diffractometer (**4**), and a Rigaku RAXIS-CS imaging plate diffractometer (**6**). Each diffractometer was used with graphite-monochromated Mo Kα radiation ($\lambda = 0.710\,69$ Å). For **1**(RT), the structure was solved by heavy-atom Patterson methods using the SAPI91 program[11] and expanded using Fourier techniques.[12] For **3**−**6**, the

Table 1. Crystallographic Data for (a) $\{[M_2(azpy)_6(H_2O)_5]\cdot 4PF_6\cdot azpy\cdot H_2O\}_n$ (M = Ni^{II} (**1**) and Co^{II} (**2**)) and (b) $\{[Zn(azpy)_3(H_2O)_2]\cdot 2PF_6\cdot 2azpy\cdot 4H_2O\}_n$ (**3**), $\{[Ag(azpy)]\cdot PF_6\}_n$ (**4**), $\{[Mn(NCS)_2(azpy)_2]\cdot azpy\}_n$ (**5**), and $\{[Ni(NCS)_2(azpy)_2]\cdot 3toluene\}_n$ (**6**)

(a) Data for **1** and **2**

param	**1**(RT)	**1**(LT)	**2**(RT)	**2**(LT)
formula	$C_{70}H_{68}F_{24}N_{28}Ni_2O_6P_4$	$C_{70}H_{68}F_{24}N_{28}Ni_2O_6P_4$	$C_{70}H_{68}Co_2F_{24}N_{28}O_6P_4$	$C_{70}H_{68}Co_2F_{24}N_{28}O_6P_4$
fw	2094.75	2094.75	2095.21	2095.21
lattice	triclinic	triclinic	triclinic	triclinic
a, Å	11.702(8)	11.635(4)	11.736(5)	11.663(4)
b, Å	17.859(10)	17.631(7)	17.878(6)	17.627(6)
c, Å	10.587(2)	10.580(4)	10.615(4)	10.656(3)
α, deg	105.25(4)	105.17(1)	105.07(1)	104.96(1)
β, deg	90.43(6)	90.06(2)	90.26(1)	89.88(1)
γ, deg	83.17(5)	83.11(1)	83.10(1)	83.03(1)
V, Å^3	2117(2)	2078(1)	2134(1)	2099(1)
space group	$P\bar{1}$ (No. 2)	$P\bar{1}$ (No. 2)	$P\bar{1}$ (No. 2)	$P\bar{1}$ (No. 2)
Z	1	1	1	1
ρ(calcd), g cm^{-3}	1.642	1.673	1.630	1.657
F(000)	1064.00	1064.00	1062.00	1062.00
μ(Mo Kα), cm^{-1}	6.43	6.55	5.85	5.95
diffractometer	AFC7R	RAXIS-RAPID	RAXIS-RAPID	RAXIS-RAPID
radiatn *λ*, Å	0.710 69	0.710 69	0.710 69	0.710 69
temp, °C	25	−180	20	−180
R ($I > 2.00\sigma(I)$)[a]	0.063	0.069	0.080	0.072
R_w (all data)[b]	0.095	0.105	0.201	0.110
no. of observs	7996 (all data)	9437 (all data)	9650 (all data)	9503 (all data)
no. of variables	671	651	676	661

(b) Data for **3**−**6**

param	**3**	**4**	**5**	**6**
formula	$C_{50}H_{52}F_{12}N_{20}O_6P_2Zn$	$C_{10}H_8AgF_6N_4P$	$C_{32}H_{24}MnN_{14}S_2$	$C_{43}H_{40}NiN_{14}S_2$
fw	1384.40	437.03	723.69	819.68
lattice	monoclinic	monoclinic	monoclinic	monoclinic
a, Å	17.207(4)	8.281(2)	11.593(2)	13.6831(6)
b, Å	13.523(3)	13.264(1)	13.641(2)	20.656(1)
c, Å	27.951(6)	13.406(4)	22.511(2)	16.3573(8)
β, deg	101.114(10)	107.51(2)	101.40(1)	110.346(2)
V, Å^3	6381(9)	1404.3(5)	3489.8(8)	4334.7(3)
space group	*C*2/*c* (No. 15)	$P2_1/c$ (No. 14)	*P*2/*n* (No. 13)	*C*2/*c* (No. 15)
Z	4	4	4	4
ρ(calcd), g cm^{-3}	1.441	2.067	1.377	1.256
F(000)	2832.00	848.00	1484.00	1712.00
μ(Mo Kα), cm^{-1}	5.32	16.13	5.43	5.86
diffractometer	RAXIS-RAPID	RAXIS-IV	AFC7R	RAXIS-CS
radiatn *λ*, Å	0.710 69	0.710 69	0.710 69	0.710 69
temp, °C	20	25	25	−100
R ($I > 2.00\sigma(I)$)[c]	0.080	0.069	0.062	0.089
R_w (all data)[d]	0.246	0.100	0.086	0.116
no. of observns	7307 (all data)	2407 (all data)	6780 (all data)	4541 (all data)
no. of variables	431	200	465	187

[a] $R = \Sigma||F_o| - |F_c||/\Sigma|F_o|$. [b] $R_w = [\Sigma w(|F_o| - |F_c|)^2/\Sigma wF_o^2]^{1/2}$. [c] $R = \Sigma||F_o| - |F_c||/\Sigma|F_o|$. [d] $R_w = [\Sigma w(|F_o| - |F_c|)^2/\Sigma wF_o^2]^{1/2}$.

structures were solved by direct methods using the SIR92 (**3** and **4**),[13] SHELXS86 (**5**),[14] and SIR97 (**6**) programs[15] and expanded using Fourier techniques.[12] For **1**(LT), **2**(RT), and **2**(LT), the structures were solved by using the final atomic coordinates of isomorphous **1**(RT) as initial coordinates and expanded using Fourier techniques.[12] Some carbon and nitrogen atoms of the disordered azpy molecule of **1**(RT), **1**(LT), and **2**(LT) and some oxygen atoms of the water molecules of **1**(LT) and **2**(LT) were refined isotropically. In **6**, there were two crystallographically independent toluene molecules. One was defined isotropically, and the other was disordered and fixed. All other non-hydrogen atoms were refined anisotropically. All hydrogen atoms, which were placed in idealized positions, were included but not refined. The refinements were carried out using full-matrix least-squares techniques on F^2. Crystal data and details of the structure determinations are summarized in Table 1. All calculations were performed using the teXsan[16] crystallographic software package of Molecular Structure Corp.

Crystallographic data for structures reported in this paper have been deposited at the Cambridge Data Centre as supplementary publication nos. CCDC-255187 (**1**(RT)), 261187 (**1**(LT)), 261189 (**2**(RT)), 261188 (**2**(LT)), 261190 (**3**), 255188 (**4**), 256220 (**5**), and

(11) SAPI91: Fan, H.-F. *Structure Analysis Programs with Intelligent Control*; Rigaku Corp.: Tokyo, Japan, 1991.
(12) DIRDIF94: Beurskens, P. T.; Admiraal, G.; Beurskens, G.; Bosman, W. P.; de Gelder, R.; Israel, R.; J. Smits, M. M. *The DIRDIF-94 program system*; Technical Report of the Crystallography Laboratory; University of Nijmegen: Nijmegen, The Netherlands, 1994.
(13) SIR92: Altomare, A.; Burla, M. C.; Carnalli, M.; Cascarano, M.; Giacovazzo, C.; Guagliardi, A.; Polidori, G. *J. Appl. Crystallogr.* **1994**, *27*, 435.
(14) SHELXS86: Sheldrick, G. M. *Crystallographic Computing 3*; Sheldrick, G. M., Kruger, C., Goddard, R., Eds.; Oxford University Press: New York, 1985; pp 175−189.
(15) SIR97: Altomare, A.; Burla, M. C.; Carnalli, M.; Cascarano, G. L.; Giacovazzo, C.; Guagliardi, A.; Moliterni, A. G. G.; Polidori, G.; Spagna, R. *J. Appl. Crystallogr.* **1999**, *32*, 115.
(16) teXsan: *Crystal Structure Analysis Package*; Molecular Structure Corp.: The Woodlands, TX, 1985 and 1999.

256221 (**6**). Copies of the data can be obtained free of charge on application to CCDC, 12 Union Road, Cambridge CB21EZ, U.K. (fax (+44) 1223-336-033; E-mail deposit@ccdc.cam.ac.uk).

Results and Discussion

Syntheses. In this study, we used two different counteranions, NCS^- and PF_6^-. Combinations of the NCS^- anion, which has an almost linear shape and strong coordination ability to a metal ion, with metal ions have yielded coordination frameworks in the presence of azpy ligand.[6a,7b,8d−h] There has, however, been only one example of an azpy coordination polymer with the PF_6^- anion, which has a spherical shape and rather weak coordination power.[8i] Hence, we investigated metal ion dependence in coordination frameworks incorporating the azpy−PF_6^- system. Since the Cd^{II} coordination polymer $\{[Cd(azpy)_3(H_2O)_2]\cdot 2PF_6\cdot azpy\}_n$, which consists of an infinite 1-D fishbone-type chain, has been reported,[8i] other metal ions (Mn^{II}, Co^{II}, Ni^{II}, Zn^{II}, and Ag^{I}) were employed in a water/ethanol solution. In the case of Ag^{I}, a 1-D linear chain coordination polymer, which is frequently observed in Ag^{I}−bidentate ligand systems, was constructed. Other metal ions with an octahedral environment formed crystalline products. For Mn^{II}, because crystalline material and another byproduct were simultaneously obtained, we unfortunately could not determine the structure and composition of the crystals. For Co^{II} and Ni^{II}, discrete 0-D dimers were obtained in place of polymeric compounds. In the case of Zn^{II}, platelike crystals, whose structure could not be determined, were formed at room temperature. However, another crystalline product with a prismlike shape was formed with increasing reaction temperature, in addition to the former platelike product. The difference in composition between the plate- and prismlike crystals was confirmed by elemental analyses and IR measurements.[17] While the prismlike crystal had a 1-D fishbone-type chain motif similar to the Cd^{II} compound,[8i] assembled structures of the 1-D motifs of Zn^{II} and Cd^{II} were different from each other. These results indicate that a variety of structures can be obtained by changing the metal ion and/or reaction temperature in the azpy−PF_6^- system. Further work is in progress to investigate the solvent- and temperature-dependence of basic structural motifs and their assembled forms in this system.

0-D and 1-D Coordination Compounds with Azpy-Mediated Aromatic Interactions. Compounds **1** and **2** were isomorphous coordination 0-D dimers. Figure 1a shows the ORTEP view around the Ni^{II} center of **1**. The selected bond distances and angles with their estimated standard deviations for **1** and **2** are listed in Tables 2 and 3, respectively. Despite the presence of only one crystallographically independent Ni^{II} center, there were two kinds of Ni^{II} environments due to static disorder: one coordination site of the Ni^{II} center was shared by two different molecules (H_2O and azpy), each with half-occupancy (Figure 1a). One Ni^{II} center had a distorted octahedral geometry with three nitrogen atoms of unidentate azpy ligands in a facial position, two oxygen atoms of H_2O molecules, and one nitrogen atom of a bidentate azpy ligand. The other center had a similar coordination environment, but one of the unidentate azpy ligands was replaced by an H_2O molecule.

There were four kinds of azpy ligands in the crystal. The first species was a unidentate coordination type (A and A′), located cis to each other and trans to the bidentate azpy ligand and coordinated H_2O, respectively. The second was a bridging type (B), which linked neighboring Ni^{II} centers to form a 0-D dimer with a Ni···Ni separation of ca. 13.3 Å, as illustrated in Figure 1b. The third was also a unidentate coordination type (C), which displayed a remarkable form of disorder at two independent positions, as shown in Figure 1c. Such disorder was observed when the single-crystal X-ray diffraction pattern was measured at very low temperature (93 K). Moreover, high electron density was observed around the coordinating N(11) atom of the type C azpy ligand and was defined as a Ni^{II}-coordinated H_2O molecule (N(11)−O(3) distance = 0.62(1) Å). These results clearly indicated that the type C azpy ligand was not located in the central position of two Ni^{II} centers but essentially occupied two independent positions; that is, there existed static disorder. The 0-D dimers were bridged by hydrogen bonds between the coordination-free nitrogen atoms of type C azpy and the oxygen atoms of statically disordered H_2O molecules (2.74-

Table 2. Selected Bond Distances (Å) and Angles (deg) for $\{[Ni_2(azpy)_6(H_2O)_5]\cdot 4PF_6\cdot azpy\cdot H_2O\}_n$ (**1**) at 298 K

Distances					
Ni(1)−O(1)	2.093(3)	Ni(1)−O(2)	2.096(3)	Ni(1)−O(3)	2.02(1)
Ni(1)−N(1)	2.166(4)	Ni(1)−N(5)	2.119(4)	Ni(1)−N(9)	2.132(4)
Ni(1)−N(11)	2.21(1)				

Angles			
O(1)−Ni(1)−O(2)	88.7(1)	O(1)−Ni(1)−O(3)	171.2(3)
O(1)−Ni(1)−N(1)	91.9(2)	O(1)−Ni(1)−N(5)	91.4(1)
O(1)−Ni(1)−N(9)	87.4(2)	O(1)−Ni(1)−N(11)	169.1(3)
O(2)−Ni(1)−O(3)	82.9(4)	O(2)−Ni(1)−N(1)	85.5(1)
O(2)−Ni(1)−N(5)	174.1(1)	O(2)−Ni(1)−N(9)	89.9(2)
O(2)−Ni(1)−N(11)	92.0(3)	O(3)−Ni(1)−N(1)	85.0(3)
O(3)−Ni(1)−N(5)	96.7(4)	O(3)−Ni(1)−N(9)	95.1(3)
N(1)−Ni(1)−N(5)	88.6(2)	N(1)−Ni(1)−N(9)	175.4(2)
N(1)−Ni(1)−N(11)	98.9(3)	N(5)−Ni(1)−N(9)	96.0(2)
N(5)−Ni(1)−N(11)	89.0(3)	N(9)−Ni(1)−N(11)	81.8(3)

Table 3. Selected Bond Distances (Å) and Angles (deg) for $\{[Co_2(azpy)_6(H_2O)_5]\cdot 4PF_6\cdot azpy\cdot H_2O\}_n$ (**2**) at 293 K

Distances					
Co(1)−O(1)	2.118(3)	Co(1)−O(2)	2.111(3)	Co(1)−O(3)	2.07(1)
Co(1)−N(1)	2.219(4)	Co(1)−N(5)	2.164(4)	Co(1)−N(9)	2.188(4)
Co(1)−N(11)	2.23(1)				

Angles			
O(1)−Co(1)−O(2)	89.0(1)	O(1)−Co(1)−O(3)	171.6(3)
O(1)−Co(1)−N(1)	91.8(1)	O(1)−Co(1)−N(5)	91.0(1)
O(1)−Co(1)−N(9)	87.9(1)	O(1)−Co(1)−N(11)	168.4(3)
O(2)−Co(1)−O(3)	83.0(3)	O(2)−Co(1)−N(1)	85.4(1)
O(2)−Co(1)−N(5)	173.5(1)	O(2)−Co(1)−N(9)	90.3(1)
O(2)−Co(1)−N(11)	92.3(3)	O(3)−Co(1)−N(1)	85.1(3)
O(3)−Co(1)−N(5)	96.7(3)	O(3)−Co(1)−N(9)	94.6(3)
N(1)−Co(1)−N(5)	88.1(1)	N(1)−Co(1)−N(9)	175.7(1)
N(1)−Co(1)−N(11)	99.7(3)	N(5)−Co(1)−N(9)	96.2(2)
N(5)−Co(1)−N(11)	89.0(4)	N(9)−Co(1)−N(11)	80.6(3)

(17) Elemental analysis for platelike crystals: Anal. Calcd for $Zn(azpy)_4(PF_6)_2(H_2O)_4$ ($C_{40}H_{40}F_{12}N_{16}O_4P_2Zn$): C, 41.27; H, 3.46; N, 19.25. Found: C, 41.26; H, 3.48; N, 19.35. IR (KBr pellet) (cm^{-1}): 3430 bm, 3121 w, 2473 w, 2352 w, 2165 w, 2103 w, 1952 w, 1641 m, 1606 m, 1586 s, 1567 m, 1492 m, 1475 w, 1420 m, 1414 s, 1322 w, 1238 m, 1224 m, 1192 w, 1167 w, 1121 m, 1091 m, 1052 m, 1027 m, 1018 m, 990 w, 979 w, 965 w, 839 s, 736 w, 567 s, 558 s, 527 w, 520 m.

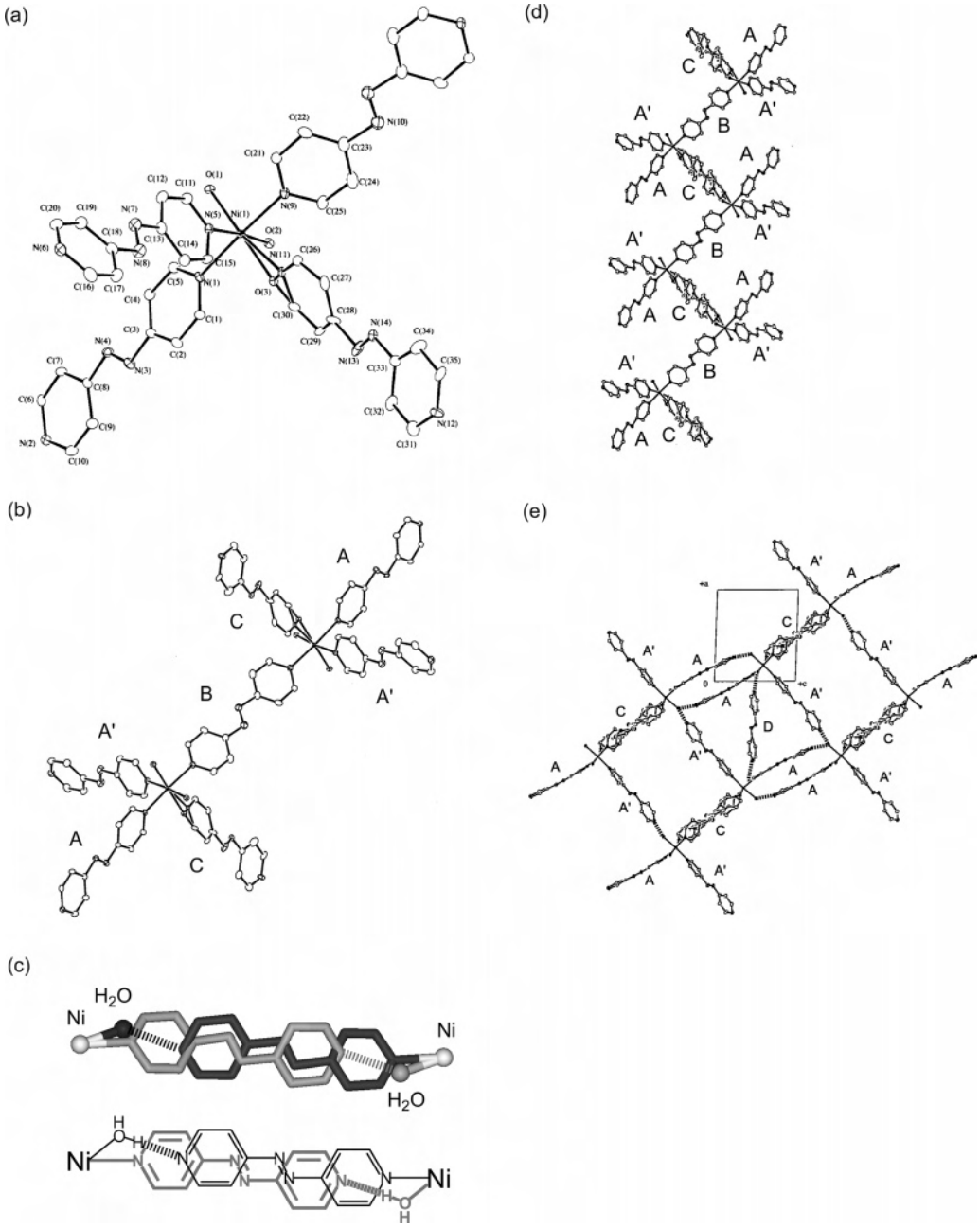

Figure 1. Crystal structure of **1**. (a, b) ORTEP views of (a) the Ni^{II} center and (b) the $Ni^{II}-Ni^{II}$ 0-D dimer at the 30% probability level. In all figures, hydrogen atoms are omitted for clarity. (c) View of the disorder mode of the type C azpy ligand and H_2O molecule between the Ni^{II} ions. The azpy and H_2O molecules have half-occupancy each. (d, e) ORTEP view of (d) the 1-D zigzag chain and (e) one 3-D supramolecular network along the *b*-axis at the 30% probability level. Dashed lines indicate hydrogen bonds. Capital letters (A, A′, B, C, and D) represent the species of azpy ligands.

(2) Å), forming a 1-D zigzag chain as illustrated in Figure 1d. Each 1-D chain was also linked by several hydrogen-bonding interactions: the free azpy ligand (the fourth type: D) bridged two coordinated H_2O molecules of neighboring 1-D zigzag chains (2.716(6) Å), and free nitrogen atoms of the unidentate azpy ligands (A and A′) interacted with coordinated H_2O molecules (2.771(6) and 2.787(6) Å, respectively). Moreover, $\pi-\pi$ and $\pi-$p interactions were observed between the type A azpy ligands (shortest atom−atom distances: 3.21 Å ($\pi-\pi$) and 3.53 Å ($\pi-$p)). These rich supramolecular interactions created a 3-dimensional (3-D) assembly as shown in Figure 1e. Two independent 3-D structures interpenetrated each other, aided by $\pi-\pi$ and $\pi-$p interactions between the type A and type C azpy ligands (shortest atom−atom distances: 3.32 Å ($\pi-\pi$) and 3.44 Å ($\pi-$p)). The PF_6^- anions were included in the vacant spaces and were hydrogen-bonded to coordinated H_2O molecules (2.832(5) Å). Free H_2O molecules were hydrogen-bonded to coordinated H_2O molecules (2.63(3) Å) and PF_6^- anions.[18]

Figure 2a shows the ORTEP drawing around the Zn^{II} center of **3**, along with the numbering scheme. Selected bond distances and angles with their estimated standard deviations

(18) There were two crystallographically independent PF_6^- anions in the crystal. The F atoms of one PF_6^- anion related to the hydrogen bond with the free H_2O molecule were intricately disordered. Therefore, the hydrogen-bonding distances were not shown.

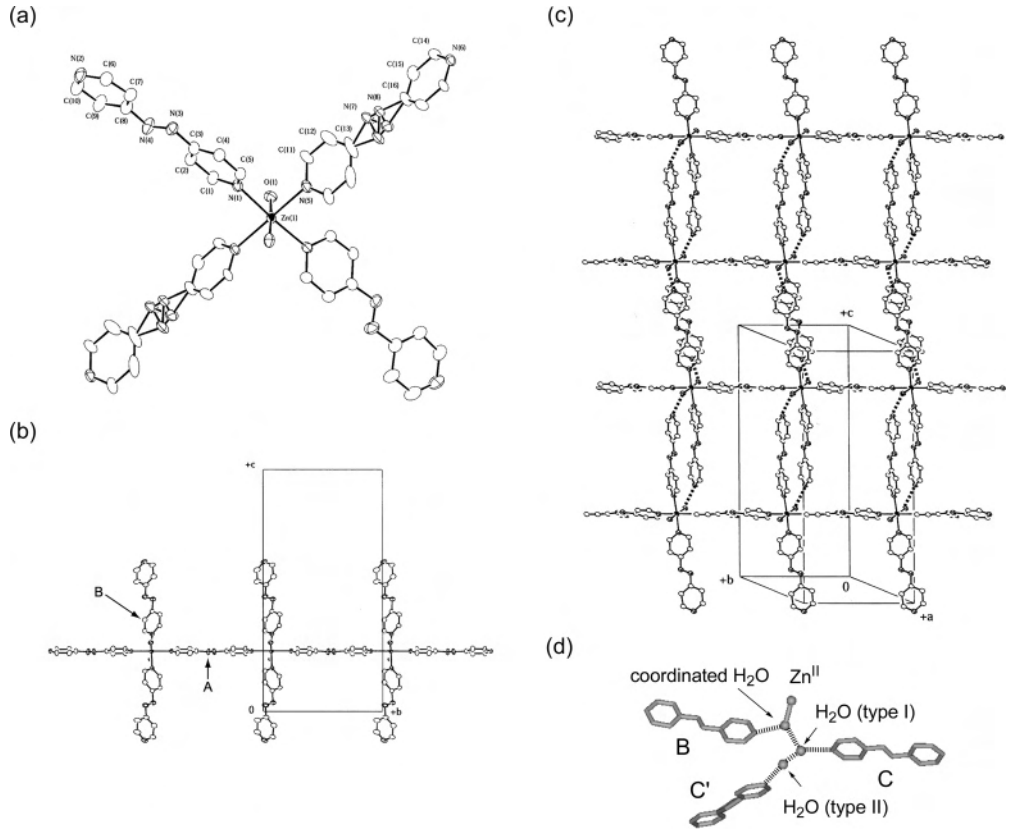

Figure 2. Crystal structure of **3**. (a−c) ORTEP view of (a) the Zn^{II} center, (b) the 1-D fishbone-type chain structure along the *a*-axis, and (c) the 2-D hydrogen-bonding assembly at the 30% probability level. (d) View of the hydrogen-bonding form between azpy ligands and H_2O molecules. Dashed lines indicate hydrogen bonds. Capital letters (A, B, C, and C′) represent the species of azpy ligands.

Table 4. Selected Bond Distances (Å) and Angles (deg) for $\{[Zn(azpy)_3(H_2O)_2]\cdot 2PF_6\cdot 2azpy\cdot 4H_2O\}_n$ (**3**)[a]

Distances					
Zn(1)−O(1)	2.092(4)	Zn(1)−N(1)	2.175(4)	Zn(1)−N(5)	2.220(6)

Angles			
O(1)−Zn(1)−O(1*)	175.5(2)	O(1)−Zn(1)−N(5)	92.2(1)
O(1)−Zn(1)−N(1)	90.0(1)	N(1)−Zn(1)−N(1*)	176.5(2)
O(1)−Zn(1)−N(1*)	90.2(1)	N(1)−Zn(1)−N(5)	88.3(1)

[a] Symmetry code: (*) $1 - x$, y, $1/2 - z$.

for **3** are listed in Table 4. The Zn^{II} ion had a compressed octahedral environment with four azpy nitrogen atoms in the basal plane and two H_2O oxygen atoms at the axial sites. There were three types of azpy ligands in this crystal. The first was a bridging type (A), which linked the Zn^{II} ions to form an infinite 1-D chain with a Zn···Zn separation of ca. 13.5 Å, and the second was a unidentate coordination type (B). These two types of azpy ligands formed a 1-D fishbone-type chain along the *b*-axis, as shown in Figure 2b. Moreover, coordination-free nitrogen atoms of the type B azpy ligands interacted with the coordinated H_2O molecules of neighboring 1-D chains via hydrogen bonds (2.812(6) Å), affording a 2-D hydrogen-bonding network with a double bridge formed by the type B azpy ligands, as illustrated in Figure 2c. Effective $\pi-\pi$ interactions between the type B azpy ligands of neighboring chains also contributed to the stabilization of the 2-D hydrogen-bonding network (shortest atom−atom distance: 3.26 Å). Free H_2O molecules participated in hydrogen bonding. One form (type I) interacted with the coordinated H_2O molecules (2.671(5) Å) and another (type II) with type I H_2O (2.742(7) Å), as shown in Figure 2d. There also existed two kinds of crystallographically independent coordination-free azpy ligands (the third type: C and C′), which acted as links between the H_2O molecules through hydrogen bonds (O(type I)···N(C) = 2.814(8) Å, O(type II)···N(C′) = 2.771(10) Å) as illustrated in Figure 2d. The type C azpy ligands further formed supramolecular $\pi-\pi$ (shortest atom−atom distance: 3.50 Å) and π−p (shortest atom−atom distance: 3.44 Å) interactions with the type B azpy ligands. The PF_6^- counteranions interacted weakly with the coordination-free H_2O (type II) by hydrogen bonds (3.005(7) Å).

Figure 3a shows the ORTEP drawing of the 1-D chain of **4** with its numbering scheme. Selected bond distances and angles with their estimated standard deviations for **4** are listed in Table 5. The Ag^I ions had two coordination sites occupied by two azpy ligands. The N−Ag−N moiety was almost linear (178.9(2)°). Ag^I atoms were linked by the azpy ligands, forming a 1-D linear chain structure along the *b*-axis with a Ag···Ag separation of ca. 13.3 Å (Figure 3a). The PF_6^- anions were weakly coordinated to the Ag^I atoms with a distance of 2.847(7) Å. The observed $\pi-\pi$ interactions mediated by azpy ligands between the chains (shortest atom−atom distance: 3.30 Å) are shown in Figure 3b.

Microporous Coordination Polymers with Aromatic Guest Incorporated by Azpy-Mediated Aromatic Interactions. Since compound **5** was prepared by reacting $Mn(ClO_4)_2\cdot 6H_2O$ and NH_4SCN with azpy in a water/ethanol

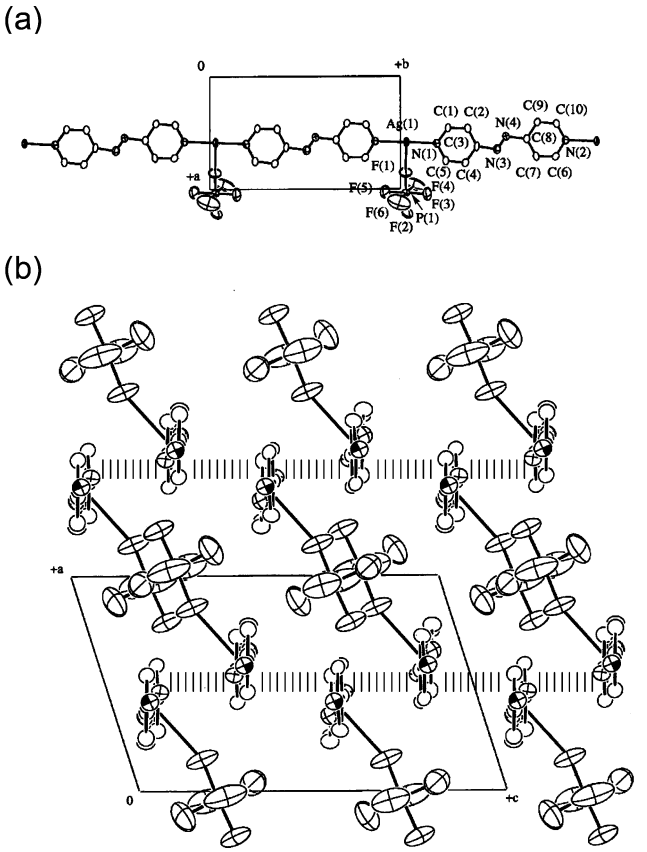

Figure 3. Crystal structure of **4**. (a, b) ORTEP view of (a) the 1-D linear chain structure along the *c*-axis and (b) the assembling structure along the *b*-axis at the 30% probability level. Dashed lines indicate $\pi-\pi$ interactions.

Table 5. Selected Bond Distances (Å) and Angles (deg) for $\{[Ag(azpy)]\cdot PF_6\}_n$ (**4**)[a]

Distances					
Ag(1)−N(1)	2.133(6)	Ag(1)−N(2*)	2.167(7)	Ag(1)−F(1)	2.847(7)

Angles			
F(1)−Ag(1)−N(1)	91.1(2)	N(1)−Ag(1)−N(2*)	178.9(2)
F(1)−Ag(1)−N(2*)	88.1(2)		

[a] Symmetry code: (*) $x, y-1, z$.

solution, there was no added aromatic guest under these reaction conditions. Therefore, the azpy molecule itself acted as an aromatic guest molecule. Figure 4a shows the ORTEP view around the Mn^{II} center of **5** with the numbering scheme. Selected bond distances and angles (with their estimated standard deviations) for **5** are listed in Table 6. Each Mn^{II} center had a compressed octahedral environment with four azpy nitrogen atoms in the basal plane and two NCS nitrogens at the axial sites. These Mn^{II} centers were linked by azpy ligands, yielding a 2-D square grid with dimensions of ca. 10×9 Å^2 (Figure 4a).[19] As shown in Figure 4b, the coordinated azpy molecules were of two kinds; in one (type A), the azpy plane was almost perpendicular to the 2-D plane, whereas the other (type B), whose azo group was disordered, was twisted by about 52° to this 2-D plane. These two different types of azpy molecules were arranged along the

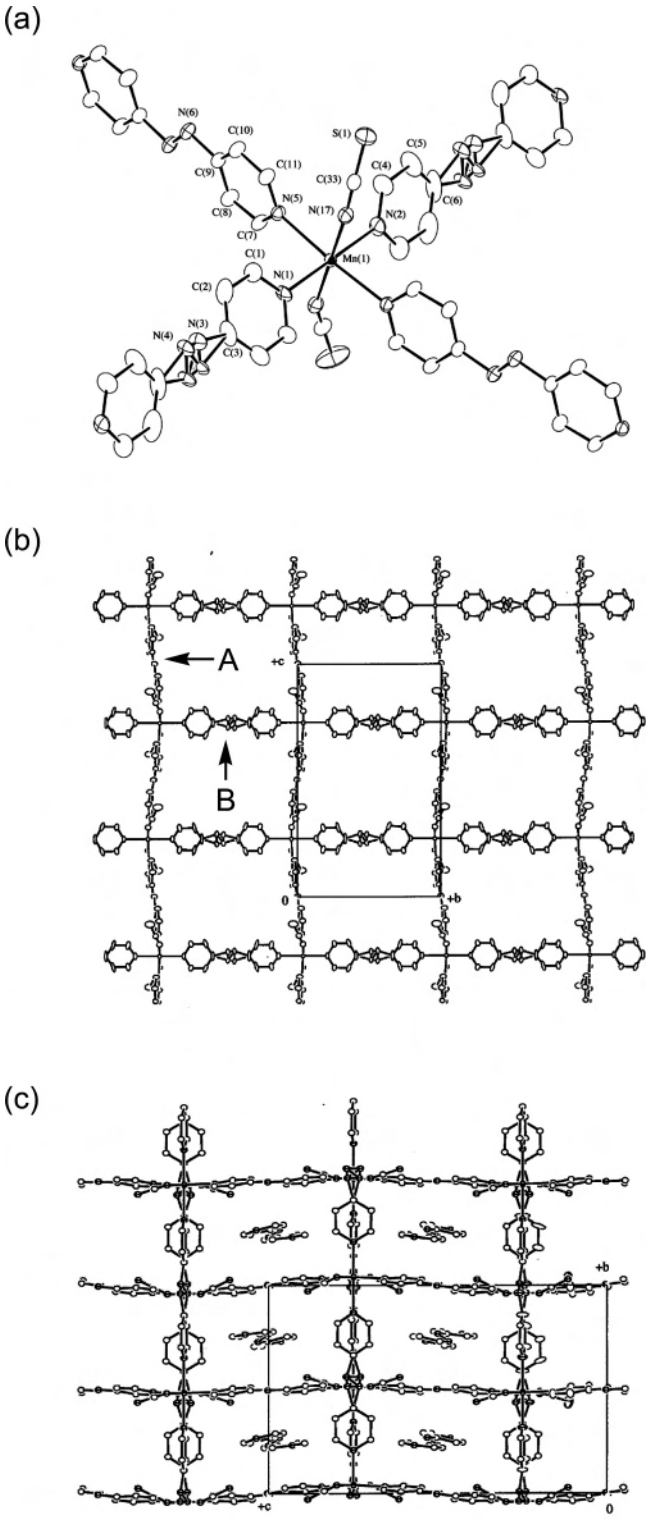

Figure 4. Crystal structure of **5**. (a−c) ORTEP drawing of (a) the Mn^{II} center, (b) the 2-D grid sheet along the *a*-axis, and (c) the microporous structure along the *a*-axis.

c- (type A) and *b*-axes (type B) in the 2-D network. The sheets were stacked so that 1-D rectangular-shaped channels were formed (ca. 5×3 Å^2) along the *a*-axis, as shown in Figure 4c, with an interlayer separation of 4.8 Å. These 1-D

(19) The size was measured by considering van der Waals radii for constituting atoms. Hereafter, all size estimations of pores were made in this way.

(20) The accessible void volume was calculated with the program PLATON by using a probe with a radius of 1.2 Å: Spek, A. L. *J. Appl. Crystallogr.* **2003**, *36*, 7.

Table 6. Selected Bond Distances (Å) and Angles (deg) for $\{[Mn(NCS)_2(azpy)_2]\cdot azpy\}_n$ (**5**)[a]

Distances					
Mn(1)−N(1)	2.301(4)	Mn(1)−N(2)	2.329(4)	Mn(1)−N(5)	2.354(3)
Mn(1)−N(17)	2.143(3)	Mn(2)−N(7)	2.312(4)	Mn(2)−N(8)	2.302(4)
Mn(2)−N(11)	2.328(3)	Mn(2)−N(18)	2.168(3)		

Angles			
N(1)−Mn(1)−N(2)	180.0	N(1)−Mn(1)−N(5)	92.48(7)
N(1)−Mn(1)−N(17)	90.23(9)	N(2)−Mn(1)−N(5)	87.52(7)
N(2)−Mn(1)−N(17)	89.77(9)	N(5)−Mn(1)−N(5*)	175.0(1)
N(5)−Mn(1)−N(17)	88.5(1)	N(17)−Mn(1)−N(17*)	179.5(2)
N(7)−Mn(2)−N(8)	180.0	N(7)−Mn(2)−N(11)	91.72(8)
N(7)−Mn(2)−N(18)	89.42(9)	N(8)−Mn(2) −N(11)	88.28(8)
N(8)−Mn(2)−N(18)	90.58(9)	N(11)−Mn(2)−N(11**)	176.6(2)
N(11)−Mn(2)−N(18)	89.7(1)	N(18)−Mn(2)−N(18**)	178.8(2)

[a] Symmetry code: (*) 1/2 − *x*, *y*, 1/2 − *z*; (**) 3/2 − *x*, *y*, 1/2 − *z*.

Table 7. Selected Bond Distances (Å) and Angles (deg) for $\{[Ni(NCS)_2(azpy)_2]\cdot 3toluene\}_n$ (**6**)[a]

Distances					
Ni(1)−N(1)	2.110(4)	Ni(1)−N(3)	2.116(4)	Ni(1)−N(5)	2.038(4)

Angles			
N(1)−Ni(1)−N(1*)	90.4(2)	N(1)−Ni(1)−N(3)	179.3(2)
N(1)−Ni(1)−N(3*)	89.8(1)	N(1)−Ni(1)−N(5)	90.1(2)
N(1)−Ni(1)−N(5*)	90.9(2)	N(3)−Ni(1)−N(3*)	90.0(2)
N(3)−Ni(1)−N(5)	89.2(2)	N(3)−Ni(1)−N(5*)	89.8(2)
N(5)−Ni(1)−N(5*)	178.5(3)		

[a] Symmetry code: (*) −*x*, *y*, 3/2 − *z*.

channels included coordination-free azpy molecules, which underwent $\pi-\pi$ (shortest atom−atom distance: 3.36 Å) and π−p (shortest atom−atom distance: 3.49 Å) interactions with the type A coordinated azpy ligands. Guest−guest interactions were not observed. Calculations from X-ray structural parameters showed that the guest-accessible void space in the channels was approximately 39%.[20] Unfortunately, the coordinated azpy molecules were removed by heating along with the guest azpy molecules in the 1-D channels, so formation of vacant channels was impossible.

Next, we tried creating a porous azpy coordination polymer with more volatile guests than azpy itself. Compound **6** was prepared by reacting $Ni(ClO_4)_2\cdot 6H_2O$ and NH_4SCN with azpy in a methanol/toluene solution. Figure 5a shows the ORTEP drawing around the Ni^{II} center of **6** with the numbering scheme. Selected bond distances and angles with their estimated standard deviations for **6** are listed in Table 7. Each Ni^{II} center had a compressed octahedral geometry with four azpy nitrogen atoms in the basal plane and two NCS nitrogens at the axial sites. The azpy ligands bridged the Ni^{II} centers to form a 2-D sheet with a rhombic grid with corner angles of ca. 76 and 103°, respectively, and dimensions of ca. 9 × 9 Å^2, as illustrated in Figure 5b. The sheets were stacked so that no effective 1-D channels were formed along the direction perpendicular or oblique to the 2-D plane. However, guest toluene molecules were lodged between the 2-D layers (channel window size: ca. 7 × 1 Å^2, 2 × 1 Å^2, and 5 × 2 Å^2 along the *c*-axis, *b*-axis, and *b*−*c* vector, respectively) as depicted in Figure 5c. Therefore, **6** had discrete cavities with small windows that prevented transfer of guest toluene molecules (minimum dimension: 4.0 and 6.6 Å).[21] The interlayer separation of 6.3 Å was considerably larger than in **5**. The azpy plane was twisted

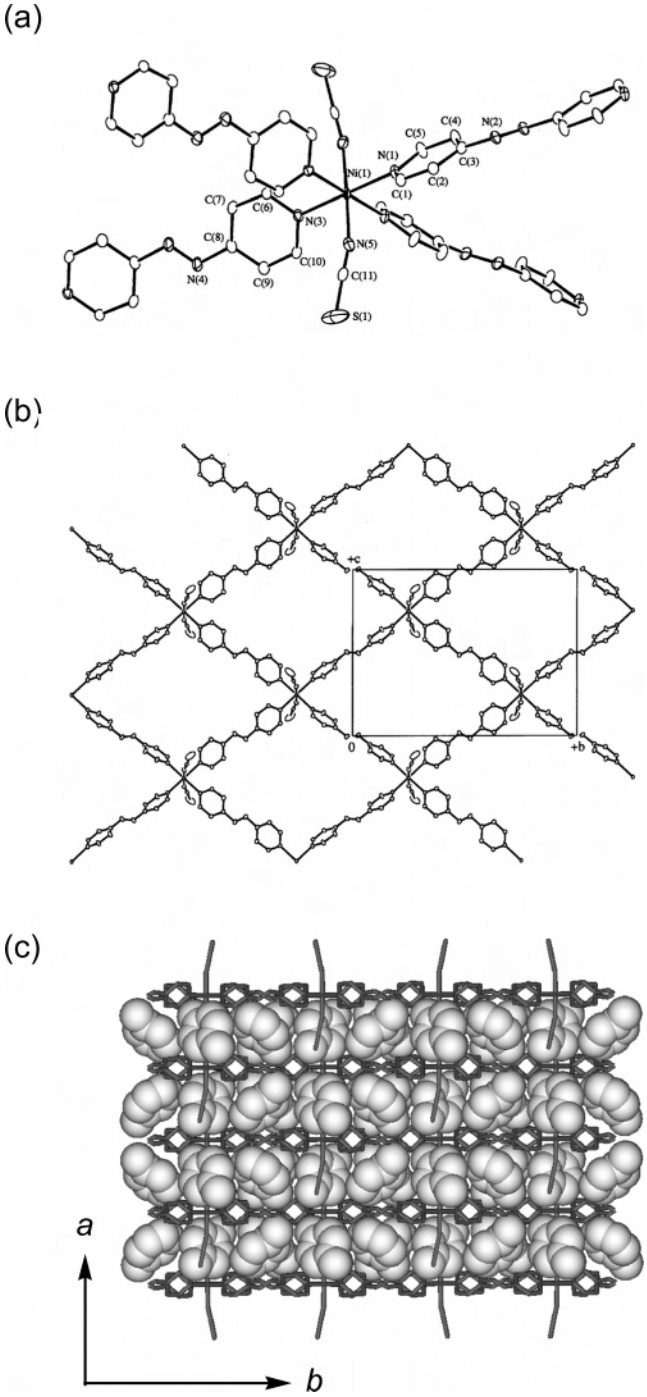

Figure 5. Crystal structure of **6**. (a, b) ORTEP drawing of (a) the Ni^{II} center and (b) the 2-D grid sheet along the *a*-axis. (c) View of the microporous structure along the *c*-axis. Guest toluene molecules are represented by CPK models.

by about 45−53° to the 2-D plane, supporting effective aromatic interactions with guest toluene molecules incorporated between the layers (vide infra). There were two crystallographically independent toluene molecules in the crystal. One was captured by $\pi-\pi$ (shortest atom−atom distance: 3.54 Å), π−p (shortest atom−atom distance: 3.36 Å), and CH−π (shortest atom−atom distance: 3.64 Å) interactions with host azpy walls. The other was loosely

(21) Webster, C. E.; Drago, R. S.; Zerner, M. C. *J. Am. Chem. Soc.* **1998**, *120*, 5509.

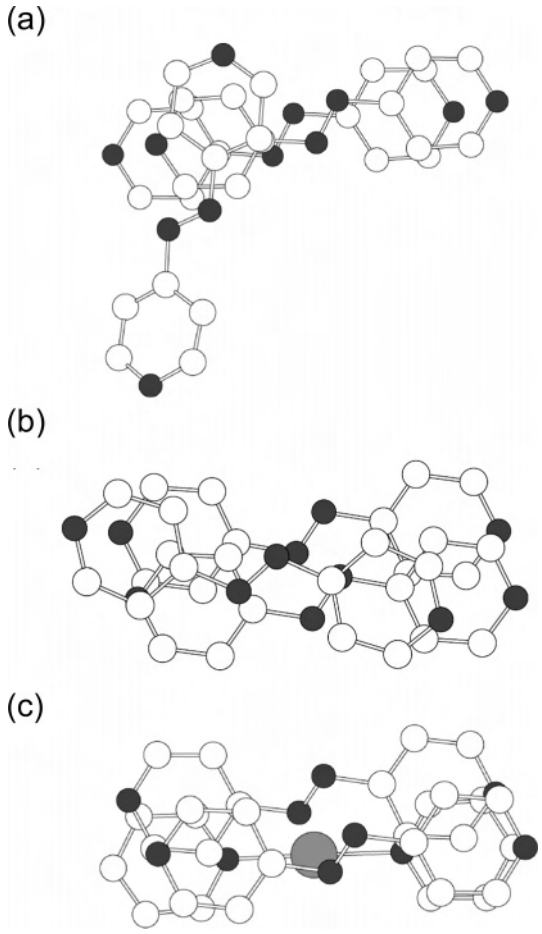

Figure 6. View of the $\pi-\pi$ and $\pi-$p overlap between the azpy ligands in **1** (a), **3** (b), and **4** (c). Small white and black circles indicate carbon and nitrogen atoms, respectively, and the large gray circle indicates a silver atom.

trapped solely by CH$-\pi$ interactions (shortest atom$-$atom distance: 3.74 Å). Guest$-$guest interactions were again not observed. Calculations from X-ray structural parameters showed that the guest-accessible void space in the channels was approximately 53%,[20] the largest of porous coordination polymers constructed with azpy building blocks, and comparable to those of the highly porous coordination polymers, $[M(AF_6)(4,4'\text{-bipyridine})_2]_n$ (M = Zn^{II} and Cu^{II}, A = Si and Ge).[22]

Interestingly, **5** and **6** did not form interpenetrated structures despite the large grids within the 2-D layers. This was probably caused by the template effect of guests incorporated by aromatic interactions.

Effective Contribution of Azpy-Mediated Aromatic Interactions to Assemblies of Low-Dimensional Motifs and Host$-$Guest Assemblies. Table 8 lists the parameters related to $\pi-\pi$ and $\pi-$p interactions in each compound. Intramolecular planarity is strongly related to facility of formation of aromatic interactions. As shown in Table 8, the intramolecular dihedral angles between the pyridine rings of the azpy ligands were ca. 0$-$10° for all our compounds except for **4**,[23] indicative of π-conjugation in the azo group leading to molecular planarity. Therefore, compounds, **1**$-$**3**, **5**, and **6** participated in a rich variety of aromatic interactions mediated by azpy ligands. In contrast, **4** had no π-conjugated structure over the azpy molecule (vide infra), although there were $\pi-\pi$ interactions between pyridine rings of the azpy ligands.

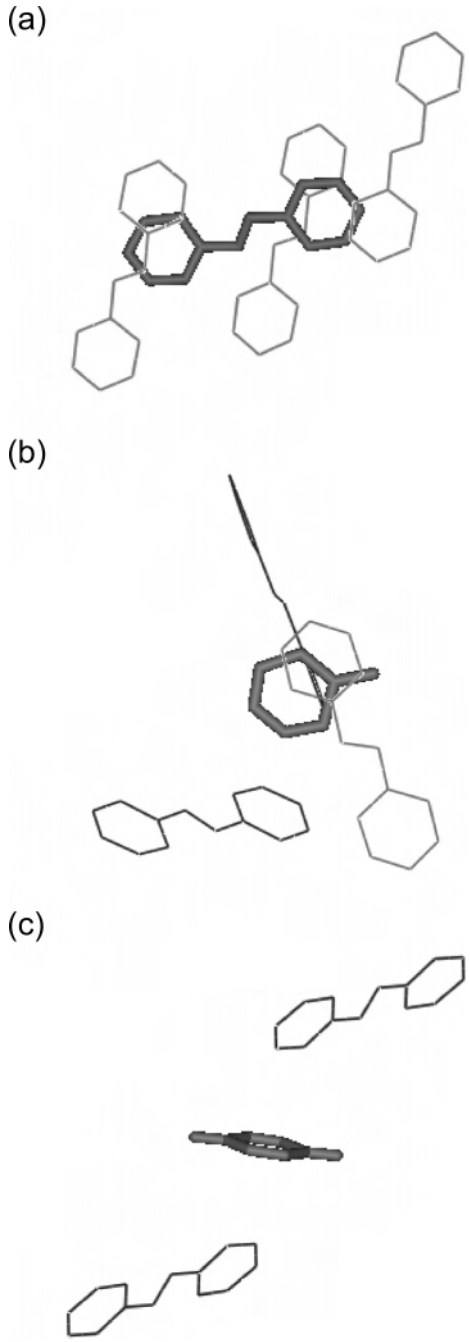

Figure 7. View of the host$-$guest aromatic interaction of (a) **5** and (b, c) **6** (b, ordered toluene; c, disordered toluene). The guest molecules are represented by sticks. The azpy molecules forming $\pi-\pi/\pi-$p and CH$-\pi$ interactions are represented by light and dark gray lines, respectively.

Figure 6 shows the overlap of azpy ligands as they relate to aromatic interactions in **1**, **3**, and **4**. As mentioned above,

(22) (a) Zaworotko, M. J. *Angew. Chem., Int. Ed.* **2000**, *39*, 3052. (b) Noro, S.; Kitagawa, S.; Kondo, M.; Seki, K. *Angew. Chem., Int. Ed.* **2000**, *39*, 2082. (c) Noro, S.; Kitaura, R.; Kondo, M.; Kitagawa, S.; Ishii, T.; Matsuzaka, H.; Yamashita, M. *J. Am. Chem. Soc.* **2002**, *124*, 2568.

(23) With one exception, the intramolecular dihedral angle of the type C azpy ligand in **1** was large (26°). This is probably because the molecular structure of the type C azpy ligand is disordered.

Table 8. Parameters Related to $\pi-\pi$ and $\pi-$p Interactions

		1(A−A)[a]	**1**(A−C)[a]	**3**(B−B)[a]	**3**(B−C)[a]	**4**	**5**	**6**
dihedral angle of two py rings (deg)	intramolecular	10	26 (C)	8	0 (C)	4	0−8	0−8
	intermolecular	10	3	8	3−5	4	9−15	14
shortest atom−atom distance (Å)	$\pi-\pi$	3.21	3.32	3.26	3.50	3.30	3.36	3.54
	$\pi-$p	3.53	3.44	*c*	3.44	*c*	3.49	3.36
centroid−centroid separation (Å)		3.49	3.46	3.72	3.94, 4.20	3.66, 3.74	3.99−4.29	4.07
shift angle (deg)[b]		16, 23	14, 16	23, 26	25−31	22−25	24−37	24, 37

[a] A−C indicate the species of the azpy ligands defined in the text. [b] Angle between the centroid−centroid vector and the normal to the π-plane. [c] No $\pi-$p interaction was observed.

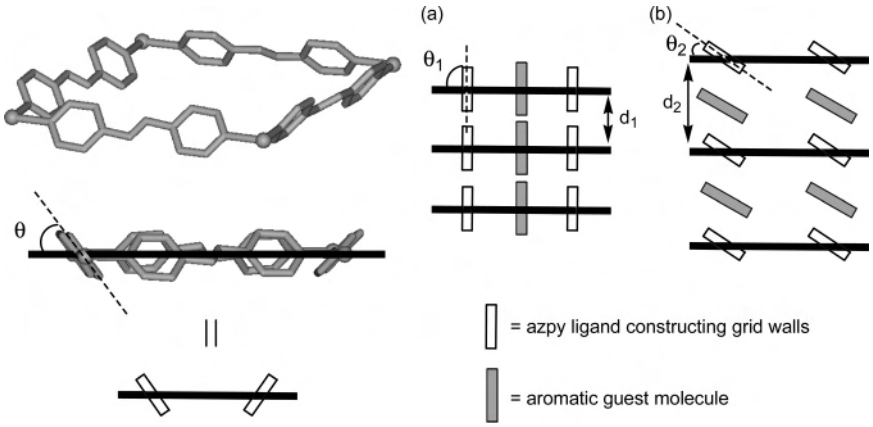

Figure 8. Schematic representation of the assembling structures of 2-D grid sheets and aromatic guests in **5** (a) and **6** (b). θ and *d* indicate a dihedral angle between pyridine rings of the azpy ligand constructing grid walls and a 2-D plane and an interlayer distance, respectively.

azpy-mediated aromatic interactions affected the assembly of their low-dimensional coordination compounds. Compounds **1** and **2** exhibited direct aromatic interactions among the 0-D dimers. There were two types of azpy stacking modes, as shown in Figure 6a. One was a parallel type, which operated between the type A azpy ligands of neighboring 0-D dimers. The other was a perpendicular type, which acted between the type A and type C azpy molecules. These were alternately arranged, forming an infinite stacking structure with a [−C−A−A−] repeating unit. The parallel type (A−A) interaction had more widespread overlap than the perpendicular type (A−C), and this difference was related to the strength of the intermolecular interaction (see Table 8). In particular, the shortest C−C bond distance of ca. 3.21 Å in the parallel type stacking indicated the presence of strong $\pi-\pi$ interactions (in general, strong interactions occur at around 3.3 Å and weaker interactions lie above 3.6 Å, with 3.8 Å being approximately the maximum contact distance for which $\pi-\pi$ interactions are accepted).[5] In compound **3**, direct aromatic interactions were observed between 1-D fishbone-type chain motifs (B−B) and via coordination-free type C azpy ligands (B−C). These interactions took place in such a way that an infinite stacking assembly with a [−C−B−B−] repeating unit was formed. All stacking azpy ligands were arranged in parallel, as shown in Figure 6b. The B−B aromatic interaction was considerably stronger than the B−C interaction, as evidenced by shortest atom−atom distances in Table 8. Compound **4**, however, had no azo-mediated $\pi-$p interaction, and only $\pi-\pi$ interactions between 1-D linear chain motifs were observed, as illustrated in Figure 6c. It is well-known that Ag^I complexes with aromatic compounds tend to form cation$-\pi$ interactions with Ag^I-C distances of 2.16−2.92 Å, with the aromatics always η^2/η^1 coordinated to the Ag^I ions.[24] In **4**, one nitrogen atom of the azo group was near the Ag^I ion with a distance of 3.236(7) Å, longer than for $Ag^I-\pi$ interactions reported up to now. This result may therefore indicate that the p electron of the azo group interacts weakly with the Ag^I ion instead of engaging in $\pi-$p interactions. The existence of the Ag^I-p interaction was also indirectly confirmed by the following result: the intramolecular dihedral angle between pyridine rings of the azpy ligand in **4** was almost planar, but each ring was not in the same plane, indicating weak π-conjugation between the pyridine and azo moieties.

In contrast with **1**−**4**, porous coordination polymers **5** and **6** formed host−guest aromatic interactions instead of aromatic interactions between frameworks. A schematic depiction of the host−guest aromatic interactions in **5** and **6** is presented in Figure 7. Compound **5** had azpy guests which did not engage in coordination or hydrogen-bonding interactions. One azpy guest interacted with three azpy ligands in the grid walls through aromatic $\pi-\pi$ and $\pi-$p interactions, as illustrated in Figure 7a. Meanwhile, **6** had two kinds of guest toluene molecules, whose modes of aromatic interaction were significantly different. One kind was incorporated by $\pi-\pi$, $\pi-$p, and CH$-\pi$ interactions (Figure 7b), whereas the other was weakly trapped by only CH$-\pi$ interactions (Figure 7c). Therefore, it was expected that the former type of guest interacted more strongly with the host azpy walls than did the latter. The results of X-ray diffraction measurements bore out this expectation: the former guest was refined isotropically, but the latter was disordered and fixed. We note here that $\pi-\pi$ and $\pi-$p interactions play an important

(24) Munakata, M.; Wu, L. P.; Ning, G. L. *Coord. Chem. Rev.* **2000**, *198*, 171.

role in the stability of a host−guest assembly. Moreover, both polymers showed different interspatial alignments of their 2-D motifs, as shown in Figure 8, despite having a similar 2-D grid sheet coordination motif. The azpy guests of **5** were located within the 2-D grids, whose pyridine rings were almost perpendicular ($\theta_1 \sim 90°$) to the 2-D plane (Figure 8a). In **6**, guest toluene molecules lay between 2-D layers with a larger layer−layer distance (d_2) than that of **5** (d_1). The pyridine rings of framework-constructing azpy ligands were twisted by ca. 45−53° (θ_2) to the 2-D plane (Figure 8b). These results implied that 2-D grid sheets with azpy building units could have guest-responsive fitting space for several aromatic guests by recognizing such guests via aromatic interactions and by regulating the dihedral angle between pyridine rings of azpy ligands and the 2-D grid sheet (θ) and interlayer distance (d).

Conclusion

The combination of an azpy ligand capable of aromatic interactions with several different metal salts has afforded the coordination compounds $\{[M_2(azpy)_6(H_2O)_5]\cdot 4PF_6\cdot azpy\cdot H_2O\}_n$ (M = Ni^{II} (**1**) and Co^{II} (**2**)) (0-D dimers), $\{[Zn(azpy)_3(H_2O)_2]\cdot 2PF_6\cdot 2azpy\cdot 4H_2O\}_n$ (**3**) (1-D fishbone-type chain), $\{[Ag(azpy)]\cdot PF_6\}_n$ (**4**) (1-D linear chain), and $\{[Mn(NCS)_2(azpy)_2]\cdot azpy\}_n$ (**5**) and $\{[Ni(NCS)_2(azpy)_2]\cdot 3toluene\}_n$ (**6**) (2-D grid sheets), which have been structurally characterized by X-ray diffraction measurements. In **1**−**3**, azpy-mediated $\pi-\pi$ and $\pi-$p interactions as well as hydrogen bonds operated between their low-dimensional (0-D (**1** and **2**) and 1-D (**3**)) coordination motifs to form 3-D assemblies. In the case of **4**, each 1-D coordination motif assembled solely through $\pi-\pi$ interactions. Compounds **5** and **6** contained microporous space, in which guest aromatic molecules were incorporated by aromatic interactions. We note that the azpy ligand with its extended π-conjugated system and p orbitals preferentially undergoes aromatic interactions such as $\pi-\pi$, CH$-\pi$, and even $\pi-$p interactions.

Our overall goal is to construct porous coordination polymers with functionalities triggered by aromatic interactions. In this study, it was confirmed that the azpy ligand employed is a good building block for the formation of several aromatic interactions not only between frameworks but also between host and guest. We expect that azpy coordination compounds will open up a new field of porous materials that can flexibly recognize and separate target guest molecules by supramolecular aromatic interactions.

Acknowledgment. S.N. expresses gratitude to RIKEN for supporting him under a Special Postdoctoral Researchers Program.

Supporting Information Available: X-ray crystallographic data for $\{[M_2(azpy)_6(H_2O)_5]\cdot 4PF_6\cdot azpy\cdot H_2O\}_n$ (M = Ni^{II} (**1**) and Co^{II} (**2**)), $\{[Zn(azpy)_3(H_2O)_2]\cdot 2PF_6\cdot 2azpy\cdot 4H_2O\}_n$ (**3**), $\{[Ag(azpy)]\cdot PF_6\}_n$ (**4**), $\{[Mn(NCS)_2(azpy)_2]\cdot azpy\}_n$ (**5**), and $\{[Ni(NCS)_2(azpy)_2]\cdot 3toluene\}_n$ (**6**) in CIF format. This material is available free of charge via the Internet at http://pubs.acs.org.

IC048371U